

Lack of time dilation in type Ia supernovae and Gamma Ray Bursts

David F. Crawford,[★]

Astronomical Society of Australia, 44 Market St., Naremburn, NSW, 2065, Australia

Accepted XXX. Received YYY; in original form ZZZ

ABSTRACT

A fundamental property of an expanding universe is that any time dependent characteristic of distant objects must appear to scale by the factor $(1+z)$. This is called time dilation. Light curves of type Ia supernovae and the duration of Gamma-Ray Bursts (GRB) are the only observations that can directly measure time dilation over a wide range of redshifts. An analysis of raw observations of 2,300 type Ia supernovae light-curves shows that their widths, relative to a standard template, have a power-law exponent as a function of $(1+z)$, of (-0.016 ± 0.038) which is consistent with no time dilation and inconsistent with standard time dilation. In addition, it is shown that the standard method for calibrating the type Ia supernovae light curves (SALT2) is flawed, which explains why this lack of time dilation has not been previously observed. Analysis of the duration of GRB shows that they are consistent with no time dilation and have very little support for standard time dilation. Consequently, this paper argues for a fundamental change from the current paradigm of an expanding universe to one for a static universe.

Key words: Cosmology: large-scale structure of the universe – Cosmology:general – Supernovae: miscellaneous

1 INTRODUCTION

Nearby type Ia supernovae are well known to have essentially identical light curves that make excellent cosmological probes. It is argued in Section 2 that the only characteristics of the light curve that change with redshift are the scaling parameters of peak luminosity and width. Here the interest is in the width which must vary with redshift in exactly the same way as time dilation. It is convenient to assume that the width dependence can be described by a parameter α where the dependence is equal to $(1+z)^\alpha$ and then to estimate α from the observations as a test of time dilation. For all current expansion models α must be one and for static models, it must be zero. Any significant difference of α from either of these two values could only be explained by a completely new cosmology.

In Section 3 it is argued that in quantum mechanics the apparent wavelength of a photon is a measurement of its energy and as a consequence its redshift may be due to any process that causes a loss of energy. Thus in quantum mechanics, the rigid nexus between the shift of spectral lines and other time variations is broken.

The observational evidence for standard time dilation has a long history with notable papers being Goldhaber

et al. (2001) and Blondin et al. (2008). The observed width of any light curve from a distant object is the product of an intrinsic width with the extra width due to time dilation. The intrinsic width is a function of the intrinsic (rest frame) wavelength which is shorter than the observed wavelength. Since many of the intrinsic wavelengths are outside the visible range, their intrinsic widths cannot be easily determined from nearby supernovae. A suitable method of solving this problem is to generate a reference template that provides a complete light curve for each intrinsic wavelength, and then to use these templates to accurately calibrate the observations by eliminating any intrinsic effects.

The SALT2 method (Guy et al. 2007, 2010) determines these templates by combining a large number of observations over a wide range of redshifts and has been used by Betoule et al. (2014), Conley et al. (2011), Foley et al. (2018), Scolnic et al. (2017) and Jones et al. (2018). In other words, the reference template is the average of the light curves from many supernovae as a function of intrinsic wavelength.

It has been first shown by Crawford (2017) and here in Section 4.1 that there is a fundamental problem with the SALT2 analysis in that a systematic variation in width as a function of redshift is included in the template as a systematic variation of the width as a function of intrinsic wavelength. The SALT2 calibration process is very good at removing the intrinsic variations but at the same time, it

★ E-mail: dcrawfrd@bigpond.net.au

removes systematic redshift variations such as time dilation. Thus supernovae light curves that have been calibrated by SALT2, or a similar method, have all the cosmological information that is a power-law function of redshift removed. In particular, any time dilation is removed from the calibrated widths.

A major part of this paper is an examination of the raw observations for 2,300 supernovae to investigate how the widths of their light curves vary with redshift. This was done separately for each filter so that observations each supernova provided up to four distinct and unrelated values for the width of the observed light curve.

The analysis is done in two stages. The first is to compare the average light curve for four different redshift ranges. The average width for these light curves are all consistent with a common value and do not have any significant dependence on redshift.

Finally, a combined fit of the light-curve widths of type Ia supernovae as a function of redshift and intrinsic width shows that the cosmological widths are proportional to $(1+z)^{(-0.016 \pm 0.038)}$ which is consistent with no time dilation and completely inconsistent with standard time dilation.

Gamma-Ray Bursts (GRB) are the only other observations that can provide direct measurements of time dilation over a wide range of redshifts. The analysis used here in Section 6 investigates the observed durations of the bursts as a function of redshift and again finds that they are consistent with no time dilation.

It is assumed for this analysis that the intrinsic properties of the type Ia supernovae light curves and the GRB burst durations are the same at all redshifts. In other words, we are assuming that there is no evolution. If there is significant evolution, it should show up in the distribution of light-curve widths with redshift. Part of this assumption for type Ia supernovae is that minor differences in the subtypes and effects of the host galaxy do not have a significant dependence on redshift. Hence their main effect is to increase the background noise.

2 COSMOLOGICAL CHARACTERISTICS OF LIGHT CURVES

Let us assume that the intrinsic radiation characteristics of type Ia supernovae are independent of redshift and that in an expanding universe the rate of universal expansion is constant for the duration of the light curve. Since cosmology only controls the transmission of the light, it follows that the shape of the received light-curve must be the same as the shape of the intrinsic light curve but with different scale factors. In other words, the cosmology can only change the peak flux density and the width of the light curve. Consequently, all of the cosmological information is contained in the dependence of these two variables with redshift. Thus, it is only necessary to measure these two scaling parameters in order to investigate the cosmology of supernovae light curves. Furthermore, we only need determine these two parameters for intrinsic light curves in order to distinguish them from cosmological effects.

Although the precise shape of the light curve is a function of intrinsic wavelength, it is assumed that the intrinsic

light-curve widths vary slowly with wavelength. Thus we can use a common light curve and measure the intrinsic width as well as the cosmological width relative to that light curve.

Since the observed light curve is the intrinsic light curve multiplied by any time dilation, then the observed width is the product of the intrinsic width and the time dilation width. We assume that the time dilation width has the power law of $(1+z)^\alpha$, where α is the exponent and has a value of one for standard time dilation. By definition, the redshift, z , is defined by $\epsilon = \lambda/(1+z)$, where λ is the observed wavelength and ϵ is the intrinsic (emitted) wavelength.

The observed wavelength is determined by the filter used and the redshift is usually measured from the observed wavelength shift of emission or absorption lines. The intrinsic width is a function of the intrinsic wavelength and we assume for this work that it has the power law ϵ^β , where β is determined by observations. Although the intrinsic light curve width almost certainly has a more complicated function of wavelength, it is only that part of it that can be described by this power law that will enable it to be confused with time dilation. Hence the model used here is that the observed width, $w(\lambda)$ is

$$w(\lambda) = (1+z)^\alpha \epsilon^\beta, \quad (1)$$

where the reference width is one. Substituting for ϵ provides the more informative equation

$$w(\lambda) = \lambda^\beta (1+z)^{(\alpha-\beta)}. \quad (2)$$

This shows the close relationship between intrinsic and cosmological power laws.

3 REDSHIFTS AND TIME DILATION

The Hubble redshift law states that distant objects appear, on average, to have an apparent velocity of recession that is proportional to their distance. Since this is consistent with models of an expanding universe in General Relativity that have universal expansion, such expanding models have become the standard cosmological paradigm. Classically, this redshift was obvious because in these models spectral lines are shifted in wavelength exactly like any other time-dependent phenomena.

However quantum mechanics tells us that light is transmitted by photons whose effective wavelength is determined from their momentum by the de Broglie equation $\lambda = hc/E$ where E is their energy and λ is their effective wavelength. Thus their effective wavelength is simply a measurement of their energy and is not a proper wavelength in the classical sense. Nevertheless it does describe how photons can be diffracted and their energy measured by an interferometer. The Doppler effect and the universal expansion are explained by an actual loss (or gain) of photon energy. A consequence is that redshifts may be due to any process that causes a loss of photon energy. Thus in quantum mechanics, the rigid nexus between the shifts of spectral lines and other time variations is broken.

4 THE INTRINSIC WAVELENGTH DEPENDENCE OF LIGHT CURVE WIDTHS

Observations of local type Ia supernovae show that the emission from the expanding gas cloud is multicoloured and the intensity is a function of both wavelength and time. A major practical problem is that the emitted wavelengths are often much shorter than the observed wavelengths and since the shape and size of the intrinsic light curve is a function of the wavelength the analysis of observations requires that this intrinsic dependence is known. For high redshift supernovae, many of the emitted wavelengths are outside the visual range, which means that we cannot, in general, use nearby supernovae to obtain the required calibrations.

An ingenious solution, exemplified by the SALT2 method (Guy et al. 2007, 2010), is to determine the calibration spectra from averaging the light curves of many supernovae at many different redshifts. Because the only observations available are from filters that cover a large wavelength range this is a difficult process. This and similar methods carefully deconstruct the average light curve, as a function of intrinsic wavelength from a large number of observations, and then generate a light-curve template for each intrinsic wavelength. Thus the light curve for any particular intrinsic wavelength will have contributions from supernovae at many observed wavelengths.

4.1 A flaw in the SALT2 method

However, there is a problem first described by Crawford (2017) with the SALT2 method of determining the characteristics of the intrinsic light curve. Let $w(\lambda)$ be the observed width at, λ , and let $W(\epsilon)$ be the width at the intrinsic (rest frame) wavelength ϵ . (The use of w and W was chosen to mimic the familiar use of m and M for magnitudes.) Similarly, let $f(\lambda, z)$ and $F(\epsilon, z)$ be the observed and emitted flux densities.

Equation 2 shows that there is a close correspondence between a systematic variation in width with intrinsic wavelength and time dilation. Although this is interesting, the extension to a wide range of wavelengths needs a more refined analysis. Here it is assumed that there is no cosmological width dependence, that is $\alpha = 0$.

The supernovae observations typically consist of the flux-density measure in filters that essentially cover the visual wavelengths. Since each filter has a filter gain function, $g(\lambda)$ which is the fraction of power transmitted per unit wavelength, then the flux density observed by a particular filter at the wavelength λ is given by

$$f(\lambda, z) \propto \int g(\lambda^*) F(\epsilon, z) d\lambda^*. \quad (3)$$

Now the width of the light curve can be determined by measuring the difference between the two half peak flux density points. To the first order this process is a linear function of the flux densities and will certainly be sufficiently linear in the last step of an iterative process of measuring the width. Thus we can apply equation 3 to the widths to get

$$w(\lambda, z) = \int g(\lambda^*) W(\epsilon) d\lambda^*. \quad (4)$$

Now suppose the intrinsic light curves have a power-law

wavelength dependence so that $W(\epsilon) = \epsilon^\beta$ where β is a constant. Then including this power law in equation 4 gives

$$w(\lambda, z) = \int g(\lambda^*) \left(\frac{\lambda^*}{1+z} \right)^\beta d\lambda^*. \quad (5)$$

Since the $(1+z)$ term is independent of λ^* it can be taken outside of the integral to get

$$w(\lambda, z) = A(1+z)^{-\beta}, \quad (6)$$

where

$$A = \int g(\lambda) \lambda^\beta d\lambda. \quad (7)$$

Clearly, A is only a function of β and the filter characteristics and it is the same for all observations with this filter. Consequently, if the intrinsic widths have a power-law dependence on wavelength, proportional to ϵ^β and from equation 6, this will be seen as a power-law dependence of the observed widths that is proportional to $(1+z)^{-\beta}$.

Conversely, if there is no intrinsic variation of the widths of the light curve with wavelength but there is a time dilation with exponent α , then the derived intrinsic wavelength dependence in the SALT2 template from multiple supernovae will have a power-law dependence with $\beta = -\alpha$.

In practice, this means that during the generation of a reference spectrum, any observed time dilation is recorded in the templates as an intrinsic wavelength dependence. When this is used to calibrate new observations that (by definition) have the same time dilation, this redshift dependence in the observations will be cancelled by the wavelength dependence in the template and the calibrated widths will be independent of redshift.

Consequently, if the SALT2 or similar calibration method is used then any cosmological information that was in the calibration observations in the form of a power law of $(1+z)$, will be removed from subsequent analyses. Simply put, the SALT2 calibration removes all power laws as function of $(1+z)$, whether artificial or genuine, leaving the calibrated light curve without any of this power-law information and therefore without any cosmological information.

4.2 SALT2 template analysis

In order to remove the expected time dilation, the first step of the SALT2 analysis is to divide all the epoch differences by $(1+z)$. If there is no time dilation, this will produce an effective time dilation of $(1+z)^{-1}$. Figure 1 shows the relative width (in blue and yellow points) for each wavelength of the widths of the light curves in the SALT2 template (cf. appendix A). Since there are clearly problems with some of the widths, shown in yellow, the analysis was confined to the blue points. The explanation for the bad widths is unknown but one contributing factor could be poor data for wavelengths between the filters. Shown in Figure 1 are some filter response curves for the nearby supernovae where this effect would be most pronounced.

The blue line is the best power-law fit of the blue points and has an exponent of $\beta = 1.240 \pm 0.011$. Then allowing for the initial division of the epoch differences by $(1+z)$ either there is no time dilation ($\alpha = 0$) and an intrinsic dependence with exponent $\beta = 0.240 \pm 0.011$, or that it has the standard

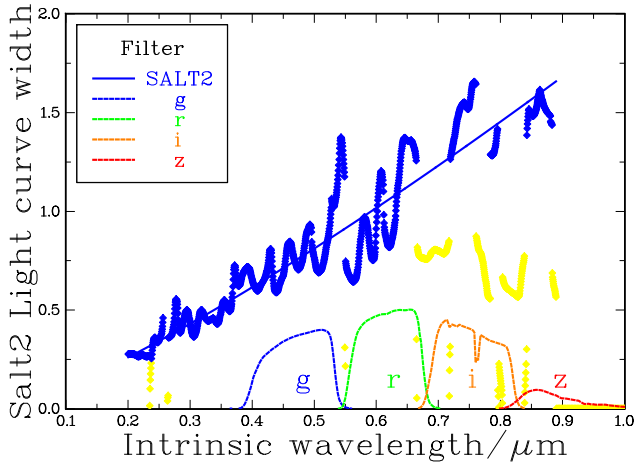


Figure 1. A plot, in blue, of the relative widths of the light curves for the SALT2 templates as a function of intrinsic wavelength. The blue line is the best fit power law with an exponent 1.240 ± 0.014 . Yellow points are assumed to be invalid. For comparison some of the filter response curves for nearby supernovae are also shown.

time dilation ($\alpha = 1$) and a large intrinsic dependence with exponent $\beta = 1.240 \pm 0.011$.

Note that if there is no time dilation and the effects of auxiliary parameters are small, then the SALT2 stretch factors are estimates of the true width.

5 TYPE IA SUPERNOVAE LIGHT CURVES

5.1 The reference template

The essential aim of this analysis is to determine α and β in equation 1, by examining the raw observations of type Ia supernovae. A critical part of any investigation into type Ia supernovae light curves is to have a reference template. Although the shape of the template is clearly dependent on intrinsic wavelength, it has been argued that the effects of time dilation do not change its shape: they only change the scaling parameters. Thus all we require from the intrinsic properties of the light curve is the width and peak flux density as a function of intrinsic wavelength in order to distinguish intrinsic properties from cosmological properties.

Although I could use an average template from the raw supernovae data, I decided that in order to remove any possible bias, it would be better to use a standard independent template, the *B* band Parab-18 from Table 2 Goldhaber et al. (2001) which has a half-peak width of 22.3 days. Then my procedure is (for each supernova) to determine the observed width of the light curve for each filter and then independently estimate α and β from all the widths as a function of redshift.

5.2 The raw observations

Crawford (2017) describes the selection and analysis of the original observations of type Ia supernovae light curves that have been selected by Betoule et al. (2014), who have provided an update of the Conley et al. (2011) analysis with

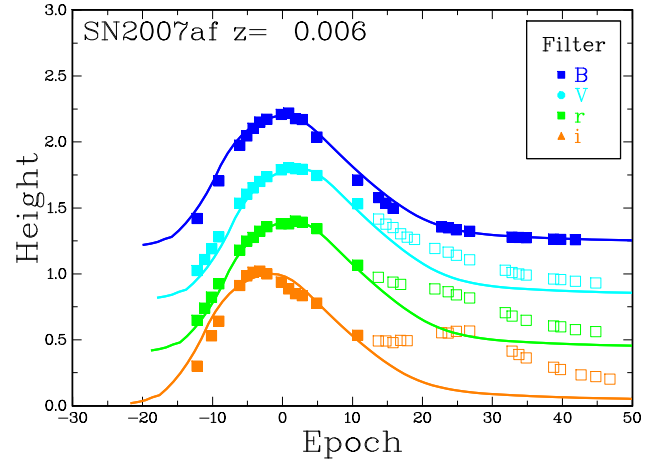


Figure 2. The light curves for the SNLS type Ia supernova SN2007af. Valid points are shown as full squares and invalid points as open squares. To avoid confusion, the filter results have been vertically displaced. The secondary peak is clearly apparent.

better optical calibrations and more supernovae. This JLA (Joint Light-curve Analysis) list sample has supernovae from the Supernova Legacy Survey (SNLS), nearby supernovae (LowZ), the Sloan Digital Sky Survey (SDSS) (Holtzman et al. 2008; Kessler et al. 2009) and those observed by the (HST) (Hubble Space Telescope) (Riess et al. 2007; Jones et al. 2013). Also included are 1169 supernova from the Pan-STARRS supernova survey (Kaiser et al. 2010; Jones et al. 2018; Scolnic et al. 2018). The sources of the raw observations are listed in the appendix A.

For each type Ia supernova, the data used here was, for each filter, a set of epochs with calibrated flux densities and uncertainties. The observations taken with the *U* and *u* filters are very noisy, and following Conley et al. (2011) and Betoule et al. (2014), the observations for these filters were not used.

5.3 The analysis of raw observations

Figure 5.3 shows the light curves for four filters for the SNLS supernova SN2007af with the filters used being shown in the legend (Goobar & Leibundgut 2011). Accepted data points are shown as solid squares whereas the rejected points are shown with an open square.

The first feature to notice is that the epoch of the peak flux density depends on the filter type and is therefore a function of the intrinsic wavelength. Secondly, there is a secondary peak at about 25 days after the first peak for the longer wavelength filters. Although this second peak is intrinsic to the supernova, it does not appear to be very consistent (Elias et al. 1981; Meikle & Hernandez 2000; Goobar & Leibundgut 2011). Consequently, as shown in Figure 5.3, all filters, except *B*, *j*, and HST, had their epochs more than 12 days after the main peak rejected. Unfortunately, the direct analysis of the data to obtain the epoch of the peak flux density, the value of the peak flux density and the light curve width using a χ^2 method has an intrinsic problem in that position of the peak flux density and the width are not

independent. However the value of the peak flux density is almost independent of the width estimate.

A method that partly overcomes this problem is to use the flux densities to provide the intrinsic light curve for each filter. The first step was to estimate the value of the peak flux density using a minimum χ^2 procedure. Next the program uses the reference light curve and the ratio of the flux density to the peak flux density to obtain a flux density epoch. This epoch has an uncertainty equal to the flux density uncertainty divided by the absolute value of the slope of the reference light curve at that epoch. Then a simple weighted regression of the observed epochs versus the flux density epochs provide the peak flux density offset and the width of the light curve.

There is the added bonus of providing uncertainty estimates for the parameters. However because of a wide range of width uncertainty estimates they were ignored in later analyses. Finally since there is a small dependence between peak flux density and width, the procedure was iterated until a stable width was found for each filter. Note that each supernova had separate values for the peak flux density and the width for each filter.

It was noted that for some filter data sets the uncertainties for the flux densities had a very wide range and some were unusually small. The problem is not with the large uncertainties but with the very small uncertainties, in that a single epoch could have weight a thousand times greater than other epochs. Clearly, this could lead to anomalous width estimates. For typical supernovae, each epoch is observed by the same telescope and except for events such as bad seeing on a particular night it is expected that for all the epochs for the same supernova should have similar flux density uncertainties. This problem of poor uncertainties was avoided by providing new uncertainties for each filter and supernovae that were set to be 3% of the peak flux density.

After all the parameters were estimated for a particular filter and the supernova, the flux density for each epoch was tested to see if it was an outlier. This was done by computing a value

$$l_i = f_i/f_{peak} - h_i, \quad (8)$$

where for each epoch, f_i is its flux density, f_{peak} is the peak flux density, h_i is the height of the reference light curve at that epoch, and i is its index. Then an epoch it was rejected as an outlier if the value $|l_i - \bar{l}|$, where \bar{l} is the average for all the other epochs l_i , was greater than five times the rms for all the other epochs. The epoch with the largest discrepancy was eliminated, then a full analysis was repeated and this continued until there were no more outliers. Note that this method does not use the original flux density uncertainties but it does assume that they are all equal. Out of 37,368 accepted epochs, there were 636 (1.7%) outliers.

The major selection criteria for each valid supernova was that, for each filter, there was at least one epoch less than five days from the peak epoch and one that was five days greater than the peak epoch, and that there were at least 4 valid epochs. And in order to show a reasonable fit to the light curve the width uncertainty must be greater than 0.005 and less than 0.3.

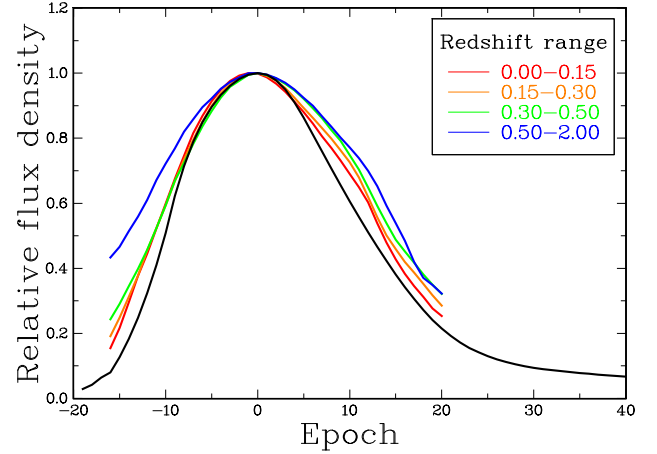


Figure 3. The type Ia supernovae light curves for four redshift ranges. The legend shows the colour for each redshift range. The template light curve is shown in black. Clearly, there is no systematic change in width with redshift.

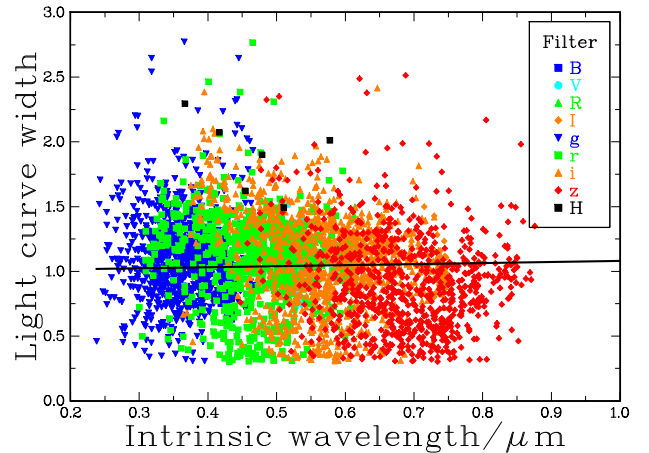


Figure 4. A plot of 3,991 type Ia supernovae filter widths as a function of intrinsic wavelength. The legend shows the filter colour and symbol of the supernovae widths for each range. The fitted power law of the intrinsic width, $e^{0.275}$, is shown in black.

5.4 Redshift dependence of light curves

The observed light curve for each of four redshift ranges was computed for each epoch in the range from -15 days to 40 days from the peak flux-density epoch. This was done by selecting all relative flux densities that were within 3 days of this epoch and setting the value of the light curve to be the median relative flux density. The median was used because it is insensitive to extreme values. This method depends only on the relative flux density for each epoch and does not depend on the fitted widths. The results are presented graphically in Figure 3 which shows the average light curve for four ranges of redshift. The black curve shows the master template light curve. Table 1 shows the redshift range, the mean redshift, the number of points, and the average width for each range. The regression of the width as a function of the average redshift gave the result

Table 1. Light curve widths for four redshift ranges

Range	\bar{z}	number	Width
0.00-0.15	0.073	25	1.125 ± 0.005
0.15-0.30	0.225	25	1.108 ± 0.008
0.30-0.50	0.383	25	1.215 ± 0.009
0.50-1.30	0.643	25	1.117 ± 0.039

Table 2. Values of fitted exponents

Row	Description	value
1	Intrinsic β	0.275 ± 0.021
2	Observed α	0.221 ± 0.039
3	Cosmological α	-0.016 ± 0.038

$width = 1.11 \pm 0.02 + (0.20 \pm 0.15)$ which is compatible with a static universe and is not compatible (5σ) with standard time dilation. Note that if there was standard time dilation the final row should have a width of 1.643.

5.5 Intrinsic widths

Figure 4 shows a plot of all 3,991 selected supernovae filter widths, as a function of their intrinsic wavelength. This is similar to the type of analysis done by Goldhaber et al. (2001) and Blondin et al. (2008). Assuming that α is zero then the weighted regression of the $\log(width)$ versus $\log(\epsilon)$ provides an estimate of the intrinsic value $\beta = 0.275 \pm 0.021$ which is in agreement with the SALT2 value (Section 4.2) of $\beta = 0.240 \pm 0.011$. Since the width uncertainties had a very large range of values this and subsequent analyses used unweighted regressions.

5.6 Cosmological widths

Because of the common redshift term (equation 2), there is a strong negative correlation between the estimates for the intrinsic width and the cosmological width. Unfortunately, a simultaneous minimisation of the observed widths for the parameters α and β in equation 2 does not work. This is because the right hand β is absorbed into the α estimate and the estimate for the remaining β will be close to zero. This is because the average width is close to one, which means that the estimate of ϵ^β will be close to one, which implies that β must be close to zero.

From Section 4.2 the intrinsic width exponent is shown in the first row of Table 2. If we assume that β is zero then the weighted regression of the $\log(width)$ versus $\log(1 + z)$ provides an estimate of the observed α which is shown in the second row of Table 2. The estimate of the cosmological α is obtained by dividing each width by $\epsilon^{0.275}$ and then redoing the regression for α with the results shown in row 3. The fact that this α is very small validates the estimate of β above.

Clearly, this cosmological α (emphasised in red) is consistent with no time dilation and completely inconsistent with standard time dilation. Furthermore these values α and β are in agreement with the SALT2 values shown in Section 4.2.

This conclusion is supported by Figure 5 which shows the distribution of these cosmological widths as a function of redshift. If there is standard time dilation, the widths should trend along the red line. For comparison Figure 6 shows what would be expected if there was standard time dilation.

5.7 A supernova with a redshift of 1.914

Jones et al. (2013) describes the observation with the HST of a supernova at a redshift 1.914. They analysed the data and found a SALT2 width of 1.367 which corresponds to a stretch factor of 0.469. It has been argued in Section 4.1 that the SALT2 method is flawed, therefore these values are flawed. My analysis of the data in their Table 1 provides widths of 2.95 ± 0.04 for the filter F125W and 2.67 ± 0.40 for the filter F160W. This result is shown in the far right of Figure 5. It should be noted that their SALT2 analysis played an important part in its identification as a type Ia supernova. Thus it may be a misidentification and its results should be treated with caution.

6 GAMMA RAY BURSTS

The website of the *Neil Gehrels* Swift Observatory, which runs the Swift satellite, that contains the Burst Alert Telescope (BAT) describes them as: “Gamma-ray bursts (GRBs) are the most powerful explosions the Universe has seen since the Big Bang. They occur approximately once per day and are brief, but intense, flashes of gamma radiation. They come from all different directions of the sky and last from a few milliseconds to a few hundred seconds.” An important characteristic of the BAT is that it has a photon counting detector (Barthelmy et al. 2005) that detects photons in the 15-150 keV energy range with a resolution of about 7 keV. It can also image up to 350 keV without position information. An important parameter for each burst is T_{90} which is a measure of the burst duration. The start and end times of T_{90} are defined as the times the fraction of photons in the accumulated light-curve reaches 5% and 95%.

The Third Swift Burst Alert Telescope Gamma-Ray Burst Catalog (Lien et al. 2016) states that “Many studies have shown that the observed burst durations do not present a clear-cut effect of time dilation for GRBs at higher redshift.” Indeed the upper panel of their Figure 25 shows that there is no obvious trend of the burst length with redshift except for a decrease in the number of short bursts with larger redshifts. This shows some support for the “tip-of-the-iceberg” effect which is sometimes used to explain the lack of strong time dilation in the GRB durations. However, there is no obvious change in the duration of longer bursts with redshift.

Now the number distribution of photons in GRB bursts is close to a power law with an exponent of about -1.6. As the redshift increases, the number of detectable photons will rapidly decrease as many photons will be below the detector limit. If we assume that the distribution of photons as a function of energy is independent of the position of the photon in the burst, then there should be no expected change in T_{90} with redshift. On the other hand, if the higher energy photons are clustered towards the centre of the GRB

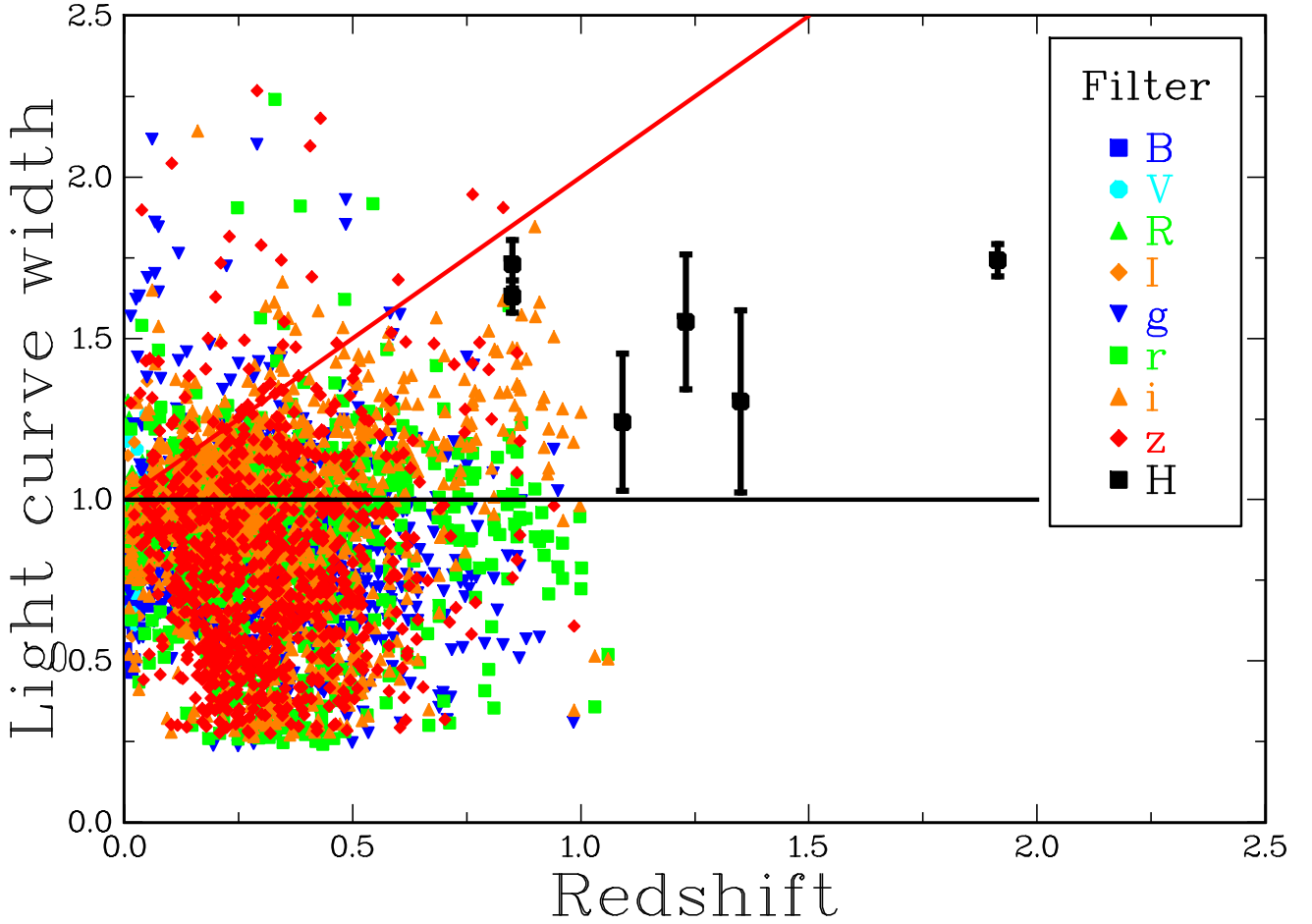


Figure 5. A plot of the measured width of the light curve for each type Ia supernova as a function of redshift. The black line shows the width for $\alpha = 0$ and the red line shows the width for standard time dilation $\alpha = 1$. The symbol and colour for each filter are shown in the legend. In order to avoid clutter only the HST observations (shown in black) have uncertainty estimates. Note that the widths displayed are limited to the range $0.4 < w < 2.5$.

then the intrinsic T_{90} should decrease with increasing redshift. Consequently, we would expect to see the normal time dilation or maybe a little less in the T_{90} measurements.

This analysis directly examines the exponent of a power-law regression of measured T_{90} of raw GRB data (c.f. Appendix B), that had burst durations above 2 seconds, as a function of $(1+z)$. Since there were no T_{90} uncertainties provided, the analysis used an unweighted regression. The power-law fits were done for the T_{90} duration with the exponent shown in row 1 of Table 3 which is consistent with no time dilation. The problem with this and similar analyses is that the variables have a very large scatter in values which would require very large numbers of GRB to achieve absolutely conclusive results.

In a recent analysis Zhang et al. (2013) claim that the GRB T_{90} widths are consistent with an expanding universe. They measured T_{90} in the observed energy range between $140/(1+z)$ keV and $350/(1+z)$ keV, corresponding to a fixed energy range in the intrinsic energy range of 140 – 350 keV. Their exponent for these selected is 0.94 ± 0.26 which is consistent with the standard expanding model.

My reanalysis of their raw, T_{90} widths using the data

in their Table 1, is shown in columns 2 and 3 of Table 3 and are consistent with no time dilation. The Swift and Zhang et al. (2013) unselected T_{90} widths are displayed in Figure 7. Although they have many common GRB, there are small differences in the T_{90} widths. This is because Zhang et al. (2013) have used their own analysis of the original data to get their own values for T_{90} widths. Examination of Figure 7 shows the large scatter of the T_{90} widths and it also shows that they are consistent with no time dilation and are unlikely to be consistent with standard time dilation.

My determination of the exponents of their energy selected widths as a function of $(1+z)$ is shown in rows 4 and 5 of Table 3. The unweighted result in row 4 (emphasised in red) agrees with their result. However the exponent for the weighted analysis shown in row 5 is consistent with no time dilation. The use of a “k correction” for T_{90} implies that there is an intrinsic dependence of burst duration on the photon energy. Since the BAT has a photon counting detector, any measurement of T_{90} is independent of the selected photon energies. The only restriction is that the photon energies must be within the detector limits. Thus BAT does not have the energy selection that is necessary for this “k

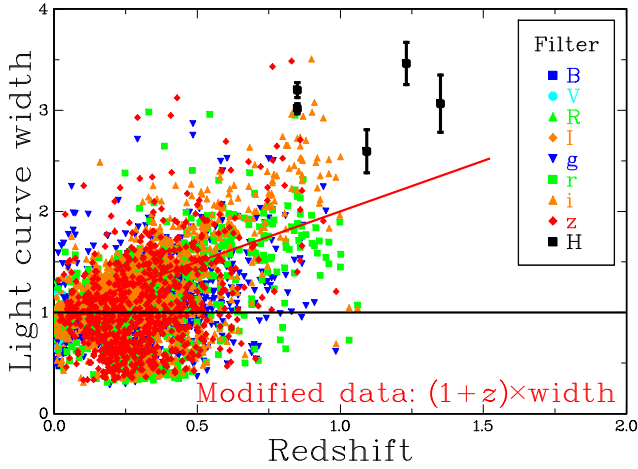


Figure 6. Same as Figure 5 except that the widths have been multiplied by $(1+z)$. This shows what the results would be if there was standard time dilation. The black line shows the width for $\alpha = 0$ and the red line shows the width for standard time dilation $\alpha = 1$. The symbol and colour for each filter are shown in the legend. In order to avoid clutter only the HST observations (shown in black) have uncertainty estimates. Note that the widths displayed are limited to the range $0.4 < w < 2.5$.

Table 3. Exponents for redshift dependence of GRB

Row	Data	Weight ^a	N	Exponent
1	Swift	U	298	0.39 ± 0.17
2	Zhang ^b	U	139	0.10 ± 0.26
3	Zhang ^b	W	139	-0.16 ± 0.20
4	Zhang ^c	U	139	0.94 ± 0.26
5	Zhang ^c	W	139	0.31 ± 0.23

^a U denotes an unweighted fit, W denotes a weighted fit

^b Raw T_{90} provided by Zhang et al. (2013) in Table 1

^c $T_{90,z}$ for intrinsic energy range of 140-350 keV.

correction”. Furthermore, it is difficult to understand how any subset of photons that are detected can have a different time dilation from the rest of the photons in the same GRB. If we ignore the energy-selected Zhang et al. (2013) results, the conclusion is that the burst length of GRB is consistent with no time dilation and has very little support for the standard model.

7 SUMMARY

7.1 Supernovae

The first part of this paper argued that the only effect of cosmology on supernovae light curves is to change the scaling parameters of peak flux density and width. The shape of the light curve is intrinsic to the supernovae and is unchanged by cosmology.

Next, it was argued that the redshift of photons is a measure of their energy and could be caused by any systematic energy loss or by time dilation.

In Section 4.1 and 4.2 it has been shown that there

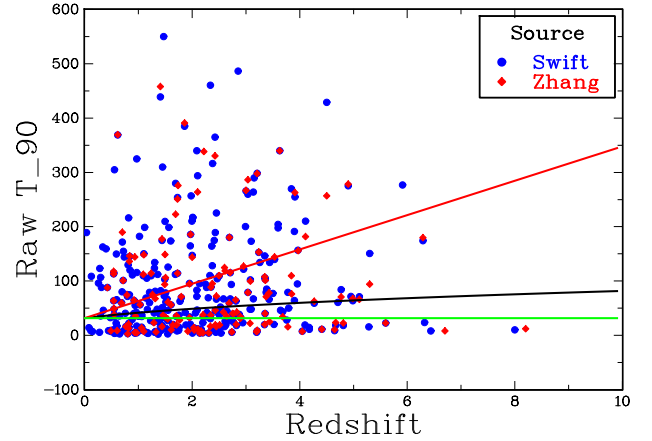


Figure 7. A plot of T_{90} as a function of redshift. The green line shows the line for no time dilation, the red line shows the line for standard time dilation, and the black line shows a time dilation with the fitted exponent of 0.39. The Swift data are shown in blue filled circles and the Zhang (Zhang et al. 2013) data are shown as red diamonds.

is a major problem in using SALT2, and similar calibration methods, to remove the intrinsic wavelength dependence of widths from type Ia supernovae light-curve observations. The process of generating the templates means that if the observed light curves have widths that contain the effects of time dilation, these effects are incorporated into the template. The subsequent use of the template will remove this time dilation affects whether artificial or genuine, from the new observations. Consequently, SALT2 calibrated light curves cannot contain any cosmological data that is in the form of a power law.

The next step, illustrated by Figure 3, was to get the light curves for four separate redshift ranges. Although it was necessary to analyse the filter observations for each supernova in order to get the value of the peak flux density and the width for that filter, that width was not used in getting the four light curves. Furthermore there is no systematic trend that is significant and consistent with standard time dilation.

Analysis of the cosmological widths as a function of redshift showed that they had a power-law exponent of $\alpha = -0.016 \pm 0.038$ which is consistent with no time dilation and is inconsistent with standard time dilation. Furthermore these values for α and β are in agreement with the SALT2 values shown in Section 4.2.

One way to validate these conclusions would be to redo the SALT2 analysis without the initial division of the epoch differences by $(1+z)$.

7.2 Gamma ray bursts

It has been shown that out to a redshift of $z = 8$, the GRB time duration variable T_{90} is consistent with no time dilation but, because of the very large scatter of values, this result cannot completely exclude the possibility of time dilation.

Table A1. Index source files for SNANA data

file
lcmerge/LOWZ_JRK07
lcmerge/JLA2014_CSP.LIST
lcmerge/JLA2014_CfAIII_KEPLERCAM.LIST
lcmerge/SNLS3year_JRK07.LIST
lcmerge/SDSS_allCandidates+BOSS_HEAD.FITS
lcmerge/JLA2014_SNLS.LIST
lcmerge/JLA2024_HST.LIST
lcmerge/SDSS_HOLTZ08

8 CONCLUSION

The final conclusion is that there is no support for an expanding universe with a standard time dilation: all the results are completely consistent with no time dilation which implies a static universe.

9 ACKNOWLEDGMENTS

This research has made use of the NASA/IPAC Extragalactic Database (NED) that is operated by the Jet Propulsion Laboratory, California Institute of Technology, under contract with the National Aeronautics and Space Administration. The calculations have used Ubuntu Linux and the graphics have used the DISLIN plotting library provided by the Max-Planck-Institute in Lindau.

APPENDIX A: SOURCE OF SUPERNOVAE OBSERVATIONS

All of the original type Ia supernovae observations were retrieved from the SNANA (Kessler et al. 2009) in the download package *snana.tar.gz* on the website <http://www.snana.uchicago.edu> using the index files shown in Table A1. A current SALT2 template file for the JLA (Joint Light-curve Analysis) analysis was taken from the SNANA website in the directory *models/SALT2/SALT2/JLAB14*.

The Pan-STARRS supernovae were accessed from the site https://archive.stsci.edu/prepds/ps1cosmo/jones_datatable.html.

Basic information for all the filters used is shown in Table A2 where column 1 is the filter name, column 2 is the mean wavelength in μm , column 3 (N) is the final number of supernovae with a valid light curve for this filter, and column 4 is the HST filter name.

APPENDIX B: SOURCE OF GRB OBSERVATIONS

The raw GRB data was taken from <https://swift.gsfc.nasa.gov/archive/grb-table> that had burst durations longer than 2 seconds and valid measurements for the redshift, T_{90} , the fluence and the peak one-second photon flux rate. The data labelled “Zhang” comes from Table 1 in Zhang et al. (2013).

Table A2. Filter characteristics

Name	Wavelength/ μm	N	HST
B	0.436	74	
V	0.541	77	
R	0.619	46	
I	0.750	44	
g	0.472	1283	
r	0.619	983	
i	0.750	1115	
z	0.888	1034	
0	1.068	7	F110W_NIC2
1	1.555	1	F160W_NIC2
4	0.771	2	F775W_WFPC2
9	1.250	1	F125W
10	1.250	1	F160W

REFERENCES

- Barthelmy, S. D., Barbier, L. M., Cummings, J. R., et al. 2005, *Space Sci. Rev.*, 120, 143, doi: [10.1007/s11214-005-5096-3](https://doi.org/10.1007/s11214-005-5096-3)
- Betoule, M., Kessler, R., Guy, J., et al. 2014, *A&A*, 568, A22, doi: [10.1051/0004-6361/201423413](https://doi.org/10.1051/0004-6361/201423413)
- Blondin, S., Davis, T. M., Krisciunas, K., et al. 2008, *ApJ*, 682, 724, doi: [10.1086/589568](https://doi.org/10.1086/589568)
- Conley, A., Guy, J., Sullivan, M., et al. 2011, *ApJS*, 192, 1, doi: [10.1088/0067-0049/192/1/1](https://doi.org/10.1088/0067-0049/192/1/1)
- Crawford, D. F. 2017, *Open Astronomy*, 26, 111, doi: [10.1515/astro-2017-0013](https://doi.org/10.1515/astro-2017-0013)
- Elias, J. H., Frogel, J. A., Hackwell, J. A., & Persson, S. E. 1981, *ApJ*, 251, L13, doi: [10.1086/183683](https://doi.org/10.1086/183683)
- Foley, R. J., Scolnic, D., Rest, A., et al. 2018, *MNRAS*, 475, 193, doi: [10.1093/mnras/stx3136](https://doi.org/10.1093/mnras/stx3136)
- Goldhaber, G., Groom, D. E., Kim, A., et al. 2001, *ApJ*, 558, 359, doi: [10.1086/322460](https://doi.org/10.1086/322460)
- Goobar, A., & Leibundgut, B. 2011, *Annual Review of Nuclear and Particle Science*, 61, 251, doi: [10.1146/annurev-nucl-102010-130434](https://doi.org/10.1146/annurev-nucl-102010-130434)
- Guy, J., Astier, P., Baumont, S., et al. 2007, *A&A*, 466, 11, doi: [10.1051/0004-6361:20066930](https://doi.org/10.1051/0004-6361:20066930)
- Guy, J., Sullivan, M., Conley, A., et al. 2010, *A&A*, 523, A7, doi: [10.1051/0004-6361/201014468](https://doi.org/10.1051/0004-6361/201014468)
- Holtzman, J. A., Marriner, J., Kessler, R., et al. 2008, *AJ*, 136, 2306, doi: [10.1088/0004-6256/136/6/2306](https://doi.org/10.1088/0004-6256/136/6/2306)
- Jones, D., Rodney, S. A., & Riess, A. G. 2013, in *American Astronomical Society Meeting Abstracts #221*, Vol. 221, 136.01
- Jones, D., Scolnic, D., Riess, A., et al. 2018, in *American Astronomical Society Meeting Abstracts #231*, Vol. 231, 308.06
- Kaiser, N., Burgett, W., Chambers, K., et al. 2010, in *Ground-based and Airborne Telescopes III*, Vol. 7733, 77330E
- Kessler, R., Becker, A. C., Cinabro, D., et al. 2009, *ApJS*, 185, 32, doi: [10.1088/0067-0049/185/1/32](https://doi.org/10.1088/0067-0049/185/1/32)
- Lien, A., Sakamoto, T., Barthelmy, S. D., et al. 2016, *ApJ*, 829, 7, doi: [10.3847/0004-637X/829/1/7](https://doi.org/10.3847/0004-637X/829/1/7)
- Meikle, P., & Hernandez, M. 2000, *Memorie della Societa Astronomica Italiana*, 71, 299. <https://arxiv.org/abs/astro-ph/9902056>
- Riess, A. G., Strolger, L.-G., Casertano, S., et al. 2007, *ApJ*, 659, 98, doi: [10.1086/510378](https://doi.org/10.1086/510378)
- Scolnic, D. M., Jones, D. O., Rest, A., et al. 2017, *ArXiv e-prints*. <https://arxiv.org/abs/1710.00845>
- . 2018, *ApJ*, 859, 101, doi: [10.3847/1538-4357/aab9bb](https://doi.org/10.3847/1538-4357/aab9bb)
- Zhang, F.-W., Fan, Y.-Z., Shao, L., & Wei, D.-M. 2013, *ApJ*, 778, L11, doi: [10.1088/2041-8205/778/1/L11](https://doi.org/10.1088/2041-8205/778/1/L11)